

Sustainable Resource based Hyperbranched Epoxy Nanocomposite as an Infection Resistant, Biodegradable, Implantable Muscle Scaffold

Shaswat Barua,[†] Bhaskariyoti Gogoi,[‡] Lipika Aidew,[‡] Alak K. Buragohain,^{‡,⊥} Pronobesh Chattopadhyay,[§] and Niranjana Karak^{*,†}

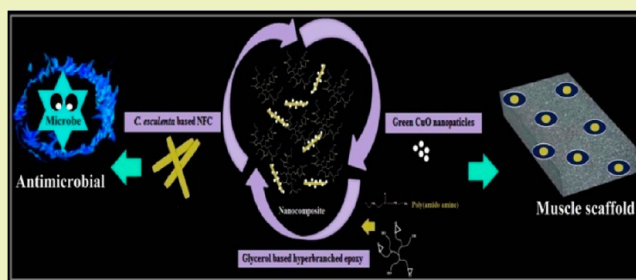
[†]Advanced Polymer and Nanomaterial Laboratory, Centre for Polymer Science and Technology, Department of Chemical Sciences, Tezpur University, Napaam, Tezpur 784028, Assam, India

[‡]Department of Molecular Biology and Biotechnology, Tezpur University, Napaam, Tezpur 784028, Assam, India

[§]Defence Research Laboratory, Tezpur 784001, Assam, India

ABSTRACT: Use of sustainable resources in the realm of materials science has opened newer possibilities for fabricating biodegradable biomaterials. Cellulose is an abundantly available bioresource that proved excellent potential in composite science and the biomaterials domain. Hence, in this report the potentiality of a “green” CuO–nanofibrillar cellulose/glycerol based hyperbranched epoxy nanocomposite was presented as an implantable muscle tissue scaffold. Muscles reconstruction has been a longstanding problem in medical science. However, with the evolution of polymeric scaffolds, repairing of damaged or lost tissues becomes possible with the aid of tissue engineering. The prepared material possessed high mechanical properties (tensile strength 55 MPa) to support cell growth. *In vitro* studies revealed that the material could support the growth and proliferation of L6 muscle cells, without causing any detriment to their cellular morphology. Further, both *in vitro* and *in vivo* toxicity assessments established the profound biocompatibility of the material. Moreover, the nanocomposite exhibited inhibitory effect against *Staphylococcus aureus*, *Escherichia coli* and *Candida albicans*, the microorganisms responsible for various surgical site infections. *In vivo* investigation revealed the biodegradability of the prepared material which overrules the need of repeated surgery for any implantable biomaterial. Thus, the overall work endorses the sustainable resource based nanocomposite as a high performance, biodegradable, antimicrobial scaffold material for reconstruction of muscles tissues.

KEYWORDS: Sustainable, Hyperbranched epoxy, Nanofibrillar cellulose, Scaffold, Antimicrobial



INTRODUCTION

With the development of materials science, many novel materials have come into focus to fulfill the ever increasing demands of mankind. During the latter part of the last century, global concern arose concurrently with the evolution of novel materials to find renewable resources for sustainable advancement of materials science. In this respect, extensive scrutiny was carried for the utility of cellulose as a multifunctional material. Recently researchers have synthesized micro and nanofibrillar cellulose from various bioresources and observed their potential utility in different fields of applications.^{1–3} We have recently isolated nanofibrillar cellulose (NFC) from the stems of *Colocasia esculenta* plant, which is commonly found in India, by using a chemical method and decorated with Cu/CuO nanoparticles.⁴ The material exhibited efficient antimicrobial activity and excellent biocompatibility with mammalian red blood cells (RBC) and peripheral blood mononuclear cells (PBMC). Again, cellulose based scaffolding is an interesting area which attained attraction for a number of biomedical applications.⁵

Scaffolds are the basic platforms for tissue engineering research. Reconstruction of damaged organs becomes possible with the aid of implantable tissue scaffolds. Skeletal muscles are voluntarily controlled strained muscle tissues, which cover the maximum part of the body. Due to trauma, burns or some congenital anomalies, these muscles may be damaged.⁶ Repairing of damaged muscles is a serious problem in medical science due to many postoperative cosmetic disorders.⁷ However, this is possible to address by the help of modern tissue engineering. Fabrication of three-dimensional polymeric scaffolds is a promising measure to culture muscle tissues *in vitro* to foster cell growth.^{8–10} Subsequent implantation of such scaffolds within host body offers clean reconstruction of muscle cells (myocytes), without inducing any cosmetic defect.

Polymeric scaffolds are advantageous in numerous ways over the conventional metal implants. They provide good

Received: January 29, 2015

Revised: April 28, 2015

Published: April 30, 2015

compatibility with the host body, overrule the necessity of repeated surgery, help in early reconstruction of tissues and most interestingly they offer tunable surface properties.^{11,12} In this context, polyester based scaffolds were prepared that showed good adhesion of smooth muscle cells (SMC).⁸ Again, polyglycolic acid (PGA) fiber based meshes were utilized to fabricate implantable device, which supported the growth of SMC.¹³ Hydrogel based scaffolds also provided good extracellular matrices for regenerating bone, cartilage and muscle tissues.¹⁴ Moreover, some materials of natural origin like collagen, elastin, fibrin etc. were exploited for muscle tissue engineering research.¹⁵ Although they are biodegradable, they provide poor mechanical strength. Further, fabrication of implantable scaffolds has challenges in overcoming the infections at surgical sites, inadequate mechanical performance and induction of toxicity to the host body, etc.¹⁶

Thus, highly compatible, infection resistant tough polymeric scaffolds are desired for tissue engineering applications to evade postsurgical complications and sound recovery of damaged tissues. In this milieu, glycerol, a biobased byproduct containing hyperbranched epoxy, was reported by our group as a tough scaffold material that showed immense potential to regenerate skin.¹⁷ Here, we report the prospect of muscle tissue regeneration by using “green” CuO–nanofibrillar cellulose/hyperbranched epoxy nanocomposite as a sustainable material. This hyperbranched epoxy, with biocompatible building blocks, offers toughness as well as good host response.¹⁸ Further, the glycerol based backbone is highly prone to degradation within the host body. Moreover; functional nanomaterials embedded in such a matrix confer fascinating biological attributes. However, the emphasis on utilization of sustainable resources motivated the researchers to explore inexpensive bioresources. Thus, here we report the preparation of a biobased hyperbranched epoxy/CuO–NFC nanocomposite for exploring such possibilities. Reported literature showcase the utility of cellulose in the fabrication of biodegradable cardiac and bone tissue scaffolds.¹⁹ The present material would be fabricated to acquire efficient antimicrobial activity by decorating CuO nanoparticles on NFC surface. This nanohybrid upon incorporation into the hyperbranched epoxy matrix would be studied as a potential sustainable scaffold for SMC regeneration.

EXPERIMENTAL SECTION

Materials. *C. esculenta* stems and the fruits of *Terminalia chebula* were collected from the University campus (Tezpur University, Assam, India). They were cut, dried and ground in a kitchen blender. Copper acetate, sodium hydroxide, glacial acetic acid and hydrogen peroxide (Merck, India) were used as received.

Preparation of the Nanocomposites. NFC was isolated from the aforementioned mass of *C. esculenta* by following our recently reported protocol with slight modification.⁴ Briefly, the mass was bleached with 7% hydrogen peroxide solution for 2 h at 45 °C, followed by sodium hydroxide treatment (5%). Finally, 50% glacial acetic acid was used to break down the cellulose fibers to smaller units. Then, the fibrils (0.5 g) were dispersed in water by using ultrasonication for 60 min to obtain the NFC. An aqueous solution of copper acetate (0.25 g in 5 mL) was added to the above dispersion and stirred for 2 h at room temperature. Then, 1 mL (4% w/v) aqueous extract of *T. chebula* fruit was added to the mixer and again stirred for 4 h at room temperature. The nanohybrid (CuNFC) was then centrifuged and washed several times with distilled water. CuNFC suspension was dried by using a lyophilizer (Labtech Freezedryer, Daihan Labtech Co. L-DF5512NFC) under high vacuum.

Hyperbranched epoxy resin was prepared by employing our reported method.²⁰ Briefly, glycerol and bisphenol A were reacted

with epichlorohydrin at 110 °C for 3 h and the resin was extracted by tetrahydrofuran (THF, SD fine Chem., India). The resin (HGE) was dried at 70 °C for 24 h.

CuNFC was dispersed in THF in three different proportions of 0.1, 0.3 and 0.5 wt % with respect to the epoxy resin separately by using ultrasonication for 1 h. Hyperbranched epoxy resin was added to each system in the mentioned ratios and magnetically stirred for 4 h at 70 °C. This was followed by 45 min of ultrasonication to allow efficient dispersion of CuNFC within the epoxy matrix. Finally, the nanocomposites were dried at 70 °C for 24 h inside a heat convection oven (Eyela, NBO-710, Japan). Three nanocomposites were coded as HGCNF1, HGCNF2 and HGCNF3 for 0.1, 0.3 and 0.5 wt % loading of CuNFC, respectively. Collectively, the three systems would be referred to as HGCNF.

Characterization. Presence of CuNFC within the nanocomposites was analyzed by a UV–visible spectrophotometer (Hitachi, U-2001, Tokyo, Japan). Chemical functionalities of the nanocomposites were detected by a Fourier transform infrared (FTIR) spectrophotometer (Impact-410 Nicolet, USA). X-ray diffractions were studied in a Miniflex X-ray diffractometer (Rigaku Corporation Japan) at the scanning speed of 2.0° min⁻¹. Distribution of CuNFC within the epoxy matrix was analyzed by the help of a transmission electron microscopy (TEM, JEOL-JEM 2100) instrument under 200 kV voltage.

HGCNF were cured by mixing them with poly(amido amine). Mechanical performance and adhesive strength of the cured nanocomposites were measured as described in our earlier report.¹⁸ Tensile strength was measured for rectangular films (60 × 10 × 0.3 mm). Again, lap shear tensile adhesive strength was determined by applying the resinous HGCNF on the interface of overlapping wood substrates (25 × 25 × 0.3 mm). All the tests were performed in triplicates and average values were considered.

Cytocompatibility Assessment. Cytocompatibility of the prepared materials was tested against wistar rat primary hepatocytes. Isolated liver was perfused in William medium (Sigma-Aldrich, Germany), enriched with 10% fetal bovine serum (FBS, Sigma-Aldrich, Germany). The cells were then cultured in the above medium for 24 h at 37 °C in an incubator under 5% CO₂ flow. Pieces of the test films (0.5 cm × 0.5 cm × 0.3 mm) were placed in a 96-well plate with the culture and the plate was incubated for 24 h. Wells without films were kept as control. Then, 40 μL of 3-(4,5-dimethylthiazol-2-yl)-2,5-diphenyltetrazolium bromide (MTT) was added to the wells. After formation of blue colored formazan crystals, DMSO (HiMedia, India) was added to the wells and UV absorbance was recorded at 540 nm. Cell survival (%) was calculated by comparing the absorbance of the treatments with that of the control.¹⁸

Adhesion of L6 Muscle Cells onto HGCNF3 Scaffold. All the cell culture materials were purchased from Sigma, USA. The cell adhesion study was performed by growing the L6 cells on HGCNF3 film. Cell adhesion was monitored by seeding L6 cells on HGCNF3 film. This was followed by inverted microscopic and SEM analysis. The L6 cell line was procured from National Centre for Cell Science, Pune, India and maintained at 37 °C under a continuous supply of 5% CO₂ using DMEM media, containing 10% FBS.²¹ Approximately 1 × 10⁵ mL⁻¹ cells were seeded in a 6-well cell culture plate, containing HGCNF3 films and were incubated for 96 h under the same condition. After termination of the incubation period, cells were observed under Axiovert A1 inverted microscope (Carl Zeiss, Germany). The media from the wells were discarded and washed three times using PBS (pH 7.4). Cells were then fixed with glutaraldehyde (2.5%) solution followed by 30 min of incubation. Excess solution was then discarded and the film was analyzed under SEM for analyzing the cell adherence on it.

Further, trypsin–EDTA solution (Sigma, USA) was used to detach the adhered cells from HGCNF3 surface and rinsed in PBS.²² Cell count was taken each day (from 0 to 4th day) of incubation by using a haemocytometer. The experiment was performed in triplicates.

In Vivo Implantation of HGCNF3 and Host Response. Implantable biomaterials require immunocompatibility with the host systems.²³ To assess *in vivo* response of the present material,

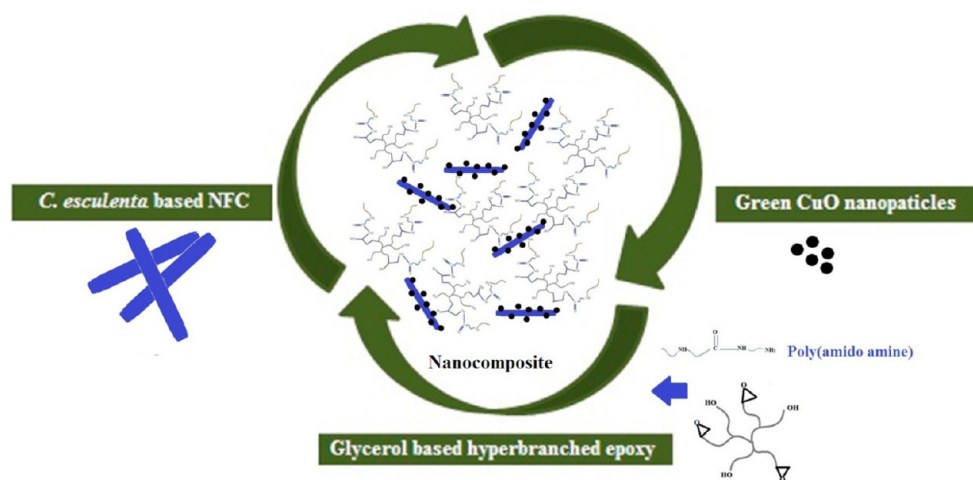


Figure 1. Schematic protocol for preparation of the nanocomposite.

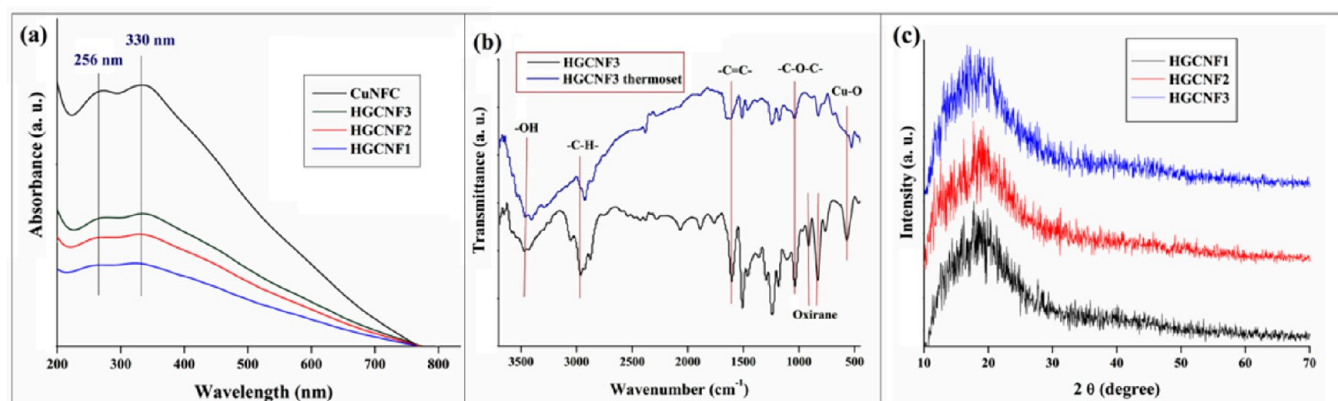


Figure 2. (a) UV–visible spectra of CuNFC and HGCNF, (b) FTIR spectra of cured and uncured HGCNF3 and (c) XRD patterns of HGCNF.

HGCNF3 was implanted within rat body (wistar male, average weight of 250–300 g). A group of animals (number, $n = 6$) was considered for the test and films were implanted subcutaneously. Another group with the same number of animals was kept as control. Immunocompatibility was analyzed by recording the hematological parameters of both the groups at 30th postimplantation day. Experiments involving animals were carried out according to the Principles of Laboratory Animal Care (NIH publication 85-23, revised 1985) with due approval from the Institutional Animal Ethics Committee.

To analyze the effect of HGCNF3 on the host tissues, histopathological study of major organs like skin, liver, kidney and brain was carried out. On 0, 15 and 30th postimplantation days, the organs were extracted and fixed with 10% formaldehyde solution and dehydrated with alcohol. Organs were embedded by paraffin and sectioned in a microtome. Sections were studied under a microscope after staining with hematoxylin and eosin.

Antimicrobial Assay. Minimum inhibitory concentrations (MIC) of CuNFC and HGCNF were determined against *Staphylococcus aureus* (ATCC 11632), *Escherichia coli* (ATCC 10536) and *Candida albicans* (ATCC 10231) to examine the effect of the materials on both Gram-positive and Gram-negative bacteria as well as on fungi. Microdilution technique was adopted to quantify the MIC, as reported in earlier work.¹⁸

The zones of inhibition for the materials were determined at their MIC against the aforementioned microbes.²⁴ Microbes were cultured in nutrient and potato dextrose broth (HiMedia, India) for 24 and 48 h respectively for bacteria and fungi. Ampicillin and nystatin were taken as the positive controls. The materials were dispersed in 1% DMSO (HiMedia, India). Then, 50 μ L of the samples were added to

the wells (8 mm diameter each) in the solidified agar plates and incubated for 24 and 48 h. The zones of inhibition were measured by a zone scale (HiMedia, India).

Again, inhibitory effect of HGCNF3 surface was studied against *S. aureus*. The bacteria was cultured for 24 h at 37 °C in nutrient broth (HiMedia, India) and centrifuged, followed by resuspension in PBS (pH = 7.4).¹⁷ Then the bacteria were again incubated in the presence of HGCNF3 film of dimension 10 × 1 × 0.3 mm, for 24 h. The film was then fixed with 2.5% glutaraldehyde solution and treated with increasing alcohol gradient (70–100%). Fate of the bacteria on interaction with HGCNF3 surface was studied by SEM.

In Vivo Biodegradation. *In vivo* biodegradability of the material was studied by implanting HGCNF3 films in wistar rats ($n = 6$). The films were sterilized with 100% ethanol and exposed to UV light for 30 min, prior to implantation. Animals were anaesthetized by injecting sodium phenobarbiton and films were implanted within subcutaneous pockets by a ventral surgery (of 20 mm). The surgical area was closed by suturing and sterilized with 70% ethanol.

After, 7, 14 and 30 days of implantation, tissue granulated scaffolds were removed by surgery and fixed with 2.5% glutaraldehyde solution. The fixed films were dehydrated using alcohol gradient and analyzed by SEM, along with unimplanted HGCNF3 film.²⁵

Statistical Analysis. Statistical evaluations were done for the obtained data by using one- and two-way ANOVA to calculate the least significant difference (LSD) among them. All the data were shown as mean \pm SD for triplicate results.

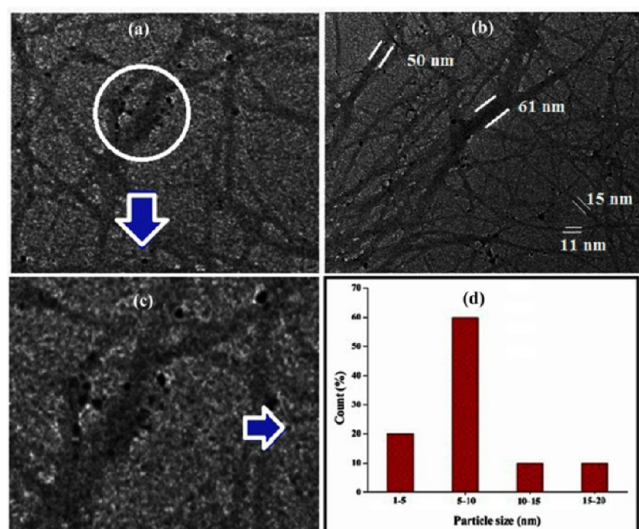


Figure 3. (a, b) Distribution of CuNFC within the matrix. (c) Enlarged area of panel a and (d) particles size distribution histogram of panel c.

Table 1. Curing Behavior, Mechanical Performance and Adhesive Strength

property	HGCNF1	HGCNF2	HGCNF3	LSD
curing time at 120 °C (min)	27.93 ± 0.4	25.83 ± 0.45	21.17 ± 0.4	0.345
swelling (%)	29.2 ± 1.08	26.47 ± 1.45	23.17 ± 1.07	0.992
tensile strength (MPa)	44.3 ± 0.86	50.7 ± 0.56	55.43 ± 0.68	0.58
elongation at break (%)	20.67 ± 0.61	18.2 ± 0.2	15.7 ± 0.2	0.318
impact resistance (m)	>1	>1	>1	
scratch hardness (kg)	>10	>10	>10	
bending (mm)	<1	<1	<1	
adhesive strength (MPa) (wood)	1233 ± 2.64	1782 ± 2	2032 ± 2	1.82

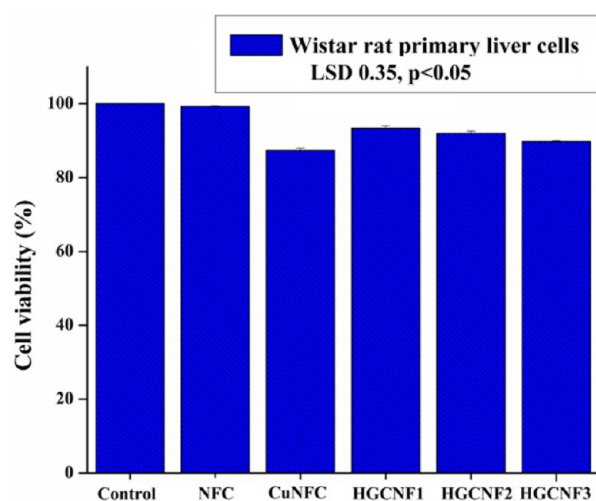


Figure 4. Cell viability percentage of rat hepatocytes.

RESULTS AND DISCUSSION

Preparation of the Nanocomposites. The ever increasing demand for advanced materials calls for exploring the utility

of sustainable bioresources in the fabrication processes.²⁶ Cellulose is a highly abundant natural feedstock, which has been used in various applications of material science.²⁷ Thus, isolation of cellulose with a cost efficient approach, can fulfill the demand of the hour. Isolation of *C. esculenta* based cellulose was thus reported by us, which put forward an easy and facile method for preparation of NFC.⁴ Further, decoration of CuO imparted excellent antimicrobial activity to the fibers. Again, the main building block of the hyperbranched epoxy is glycerol, which can be obtained from renewable resources like, vegetable oils. Thus, in this report sustainable resource based hyperbranched epoxy/CuNFC nanocomposite is prepared to fabricate a biodegradable, microbial infection resistant muscle scaffold. The difficulty in dispersing CuNFC was overcome by minimal incorporation of the nanohybrid to the matrix. Beyond 0.5 wt %, dispersion was quite difficult and a clear phase separation was observed during the cross-linking process. Figure 1 schematically represents the preparation of the nanocomposite.

Cellulose based nanoreinforcing agent was selected for the present purpose because of its compatibility with biosystems.²⁸ Further, “green” route mediated metal nanoparticles showed good biocompatibility with different cell lines as well as with *in vivo* systems.²⁹

Characterization. Presence of CuNFC in the nanocomposites was preliminarily examined with the help of UV–visible spectroscopy. Characteristic plasmon peaks for CuO were observed at 256 and 330 nm in the case of CuNFC (Figure 2a). Nanocomposites also revealed the existence of CuNFC within their matrices by exhibiting similar kind of spectral behavior. However, slight deviations were observed for the plasmon peak positions in each material.

The FTIR spectra revealed the functionalities associated with the nanocomposite (Figure 2b). The sharp band at 1047 cm⁻¹ stands for the C—O—C stretching of the pyranose ring. β-Glycosidic linkages within the glucose units of cellulose are shown by the band at 909 cm⁻¹.⁴ The band at 1607 cm⁻¹ is for the aromatic C=C stretching of cellulose units. A characteristic C—H vibration band of cellulose was witnessed at around 2979 cm⁻¹. Further, bands at 3350–3500 cm⁻¹ show the absorption of different polyphenolic compounds of *T. chebula* extract on the surface of CuNFC.⁴ Cu—O linkage was confirmed from the band at 537 cm⁻¹. Characteristic bands for oxirane ring were observed at 921 and 840 cm⁻¹ in the uncured HGCNF3. Their absence in the thermoset abundantly clarifies the successful cross-linking of the nanocomposites.

CuO nanoparticles with monoclinic lattice structure were coated onto NFC in our recent report using similar methods.⁴ Here, XRD patterns of the nanocomposites showed no distinct characteristic feature of CuNFC (Figure 2c). This is attributed to the masking effect induced by the polymeric matrix. Only 0.5 wt % loading of the nanohybrid could not show the Bragg’s lattice reflection planes for CuO and NFC. However, the broad diffraction peaks around 2θ value 21° were observed for the amorphous hyperbranched matrix.

Distribution of CuNFC within the matrix was depicted from the TEM micrographs (Figure 3). Fibers were seen with diameters, ranging from 10 to 80 nm. CuO nanoparticles were decorated over NFC in uniform manner. Particle size distribution histogram demonstrated that maximum particles lie between a size spectrum of 5–10 nm (Figure 3d). Dispersion of cellulose in polymeric system is very difficult due to high density of hydroxyl functionalities in cellulose,

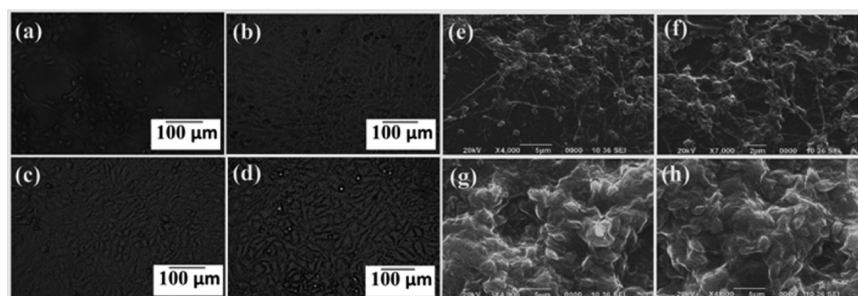


Figure 5. (a–d) Inverted microscope images of L6 cells adhered onto HGCNF3 on first to fourth day of incubation and (e–h) SEM images of L6 cells adhered onto HGCNF3 on first to fourth day of incubation.

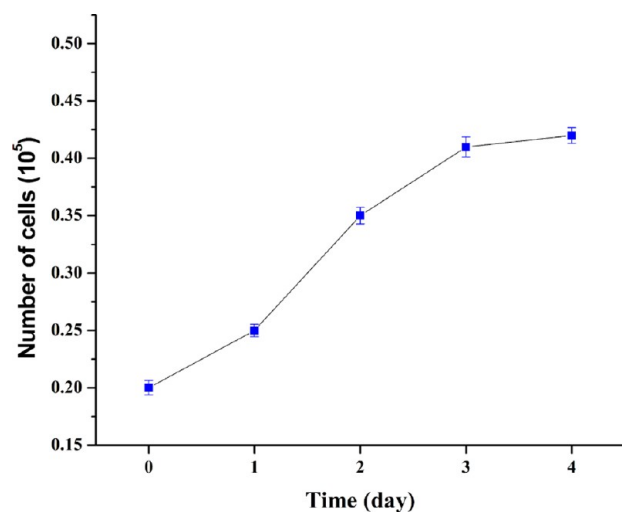


Figure 6. Growth rate of L6 cells on the surface of HGCNF3.

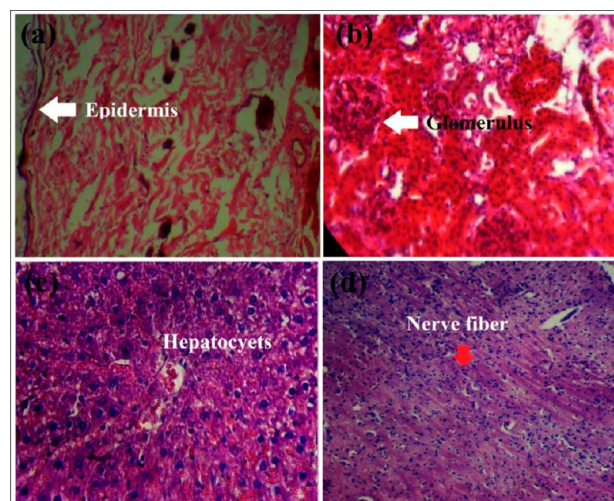


Figure 7. Histopathological sections of (a) skin, (b) kidney (c) liver and (d) brain of HGCNF3 implanted rat.

which imparts intramolecular hydrogen bonding.³⁰ However, in the present case amount of NFC is very less as compared to the matrix. This confers good dispersion of CuNFC within the epoxy system, as reflected from the TEM micrographs.

Performance of the Nanocomposites. Nanocomposites were cured at 120 °C by reacting with poly(amido amine) hardener. Cellulose possesses lots of hydroxyl groups which take part in the cross-linking reaction. Thus, curing time decreased with increase in CuNFC loading (Table 1). Effect of CuO may be minimal in the cross-linking process. Besides, functionalities of hyperbranched epoxy minimize the curing

time. Successful curing was confirmed from the swelling values, which showed 70–80% cross-linking in each case.

Tensile strength increased with the increasing amount of CuNFC in the nanocomposites (Table 1). Interaction of NFC with epoxy and poly(amido amine) functionalities forms a rigid three-dimensional network, which showed high stress bearing capacity. Again, electrostatic interaction of CuO with NFC and epoxy further aid to the increment of tensile strength. Elongation at break signifies the amount of strain the material can withstand before the point of break. Increasing amount of CuNFC decreased the elongation value to a little extent.

Table 2. Hematological Parameters of HGNFC3 Implanted Rats (on 0, 15, and 30 postimplantation days)

parameter	0 day		15 days		30 days	
	control	HGCNF3	control	HGCNF3	control	HGCNF3
Lym (%)	39.1 ± 0.18	37.5 ± 0.67	40.4 ± 1.5	39.8 ± 0.73	39.2 ± 0.78	40.2 ± 0.40
Mon (%)	19.7 ± 0.34	19.5 ± 0.54	20.3 ± 0.18	19.4 ± 0.68	20.8 ± 0.92	19.9 ± 0.63
Neu (%)	64.48 ± 0.53	63.9 ± 0.32	62.5 ± 0.52	63.4 ± 0.82	65.1 ± 0.41	64.3 ± 0.56
Eo (%)	6.2 ± 0.22	7.1 ± 0.37	7.2 ± 0.54	7.3 ± 0.12	7.9 ± 0.83	7.1 ± 0.29
Ba (%)	0.5 ± 0.19	0.6 ± 0.51	0.7 ± 0.21	0.8 ± 0.48	0.9 ± 0.78	0.9 ± 0.39
RBC (m/mm ³)	8.2 ± 0.74	8.3 ± 0.21	8.8 ± 0.23	8.1 ± 0.89	8.2 ± 0.52	8.3 ± 0.93
MCV (fl)	65.2 ± 0.89	64.7 ± 0.91	66.4 ± 0.71	64.1 ± 0.63	64.1 ± 0.83	64.1 ± 0.82
Hct (%)	43.5 ± 0.68	43.8 ± 0.81	44.2 ± 0.83	45.4 ± 0.84	46.1 ± 0.71	45.8 ± 0.48
MCH (pg)	16.2 ± 0.7	17.9 ± 0.12	17.2 ± 0.9	18.1 ± 0.62	18.8 ± 0.91	17.8 ± 0.65
MCHC (g/dL)	38.59 ± 0.3	37.1 ± 0.39	37.2 ± 0.79	39.1 ± 0.68	39.2 ± 0.15	38.9 ± 0.87
Hb (g/dL)	14.6 ± 0.56	15.1 ± 0.52	14.2 ± 0.14	15.1 ± 0.81	14.5 ± 0.89	15.8 ± 0.81
Pct (%)	0.75 ± 0.91	0.78 ± 0.73	0.76 ± 0.25	0.78 ± 0.9	0.77 ± 0.32	0.80 ± 0.54

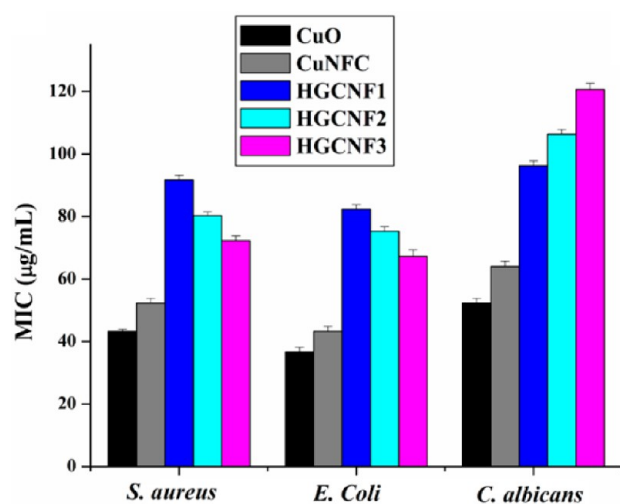


Figure 8. MIC values against *S. aureus*, *E. coli* and *C. albicans*.

However, bending test confirmed excellent flexibility of the materials, which can be folded to 180° curvature without crack. The strength and flexibility of the nanocomposites suggested that they can be used as tough scaffold materials, after assessing their bioactivities.

Adhesive strength also augmented with increase in the loading of CuNFC. Functional groups of the nanocomposites interact with the polar groups of wood by means of different secondary bonding forces. The overall mechanical study showed that formation of nanocomposite, significantly enhanced performance of the material to a significant extent over the pristine epoxy system.¹⁸

Cytocompatibility Assessment by MTT Assay. The major criterion of a sustainable material is its compatibility to human health and environment. Cellulose, being a bioresource is highly compatible with animal cell lines.²⁸ Cellulose fibers of nano dimension also proved their compatibility in different *in vitro* tests.⁴ NFC thus exhibited 99% cell viability when incubated with wistar rat primary hepatocytes (Figure 4). However, a little decrement of viable cells was observed in the case of CuNFC, which may be due to the high surface activity of the nanohybrid. Loading of CuNFC into epoxy matrix up to 0.5 wt % induced no significant toxicity to the hepatocytes. Hence, more than 89% cell survival was witnessed when incubated with the nanocomposites. The differences might be due to the variable amounts of CuNFC within the matrices. One way ANOVA revealed that cell viability percentages are

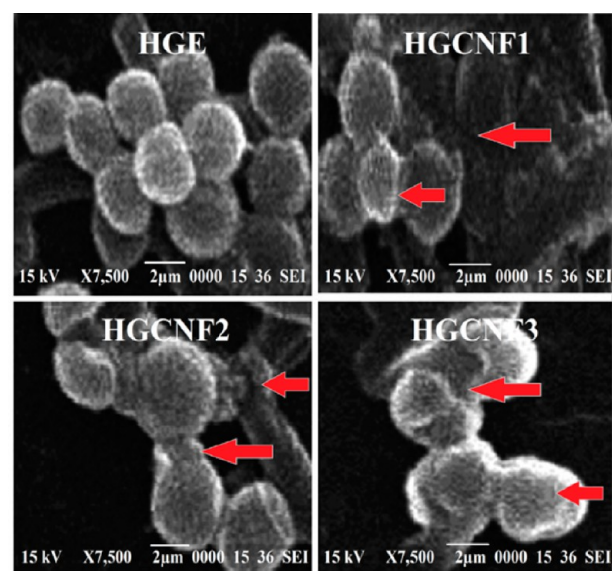


Figure 10. SEM micrographs of *S. aureus* adhered to HGE and HGCNF.

not significantly different from each other, with LSD 0.35 ($p < 0.05$). The MTT assay thus suggested that the prepared nanocomposites may have utility in advanced biomedical applications.¹⁵

Adhesion of L6 Muscle Cells onto HGCNF3 Scaffold.

Cellulose based scaffolds are explored for the reconstruction of cardiovascular, bone and skin damage.³¹ However, existing literature showcase very few reports regarding the use of cellulose based polymeric scaffolds for SMC regeneration.³² Microscopic images shows well adhered L6 cells on the HGCNF3 surface (Figure 5). No morphological alteration was witnessed for the adhered myocytes. This affirmation was further supported by the SEM micrographs where elongated myocytes were seen to be adhered on the surface of HGCNF3 (Figure 5e–h). The vital characteristics of a scaffold material are to provide mechanical toughness as well as compatible surface where cells can anchor on easily.³³ Porous structure of cellulose helps the cells to adhere on the HGCNF3 scaffold surface. Thus, HGCNF3 can provide a surface which supports the adherence and growth of myocytes, by behaving as an extracellular matrix. During the experiment, it was observed that number of adhered cells was increased with incubation time (Figure 6). This implicates that HGCNF3 surface can aid

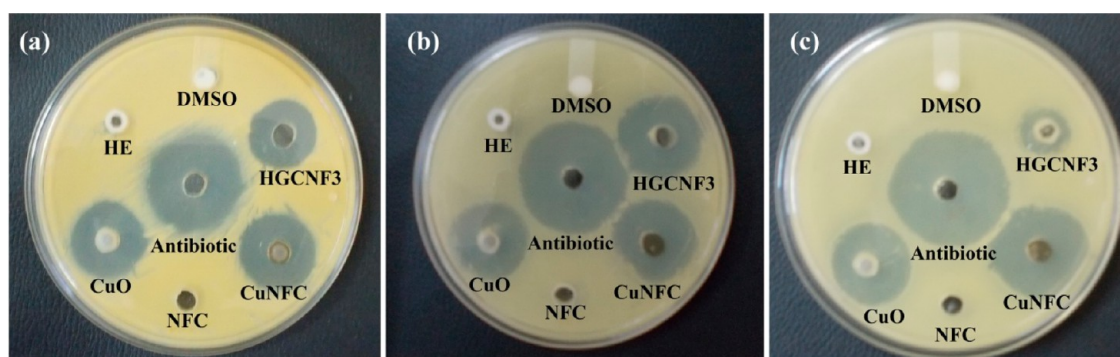


Figure 9. Zones of inhibition against (a) *S. aureus*, (b) *E. coli* and (c) *C. albicans*.

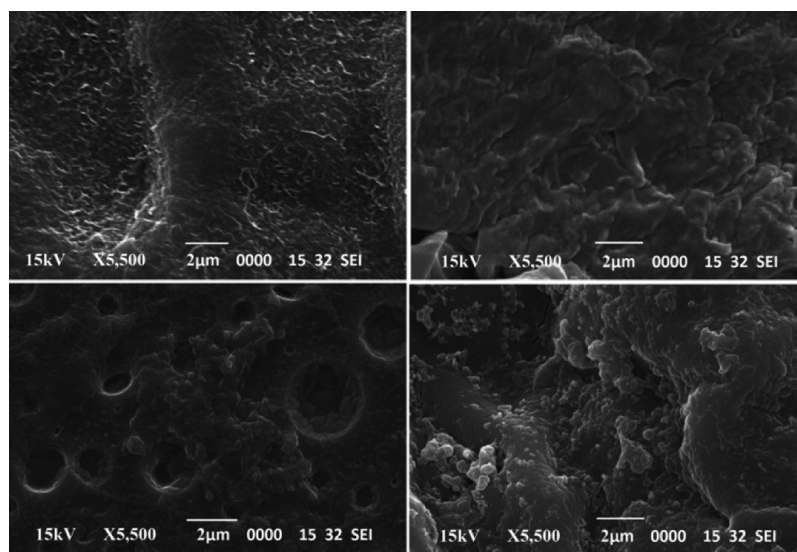


Figure 11. SEM micrographs of (a) unimplanted HGCNF3, (b–d) degradation of HGCNF3 on 7, 14 and 30 days of implantation.

to the proliferation of myocytes, without inducing any abnormality to the cells.³¹

In vivo Implantation of HGCNF3 and Host Response.

Hematological parameters govern many important physiological functions in animal body.³⁴ Abnormality to any of the parameter may lead to drastic disorder of metabolic system. The white blood cell components, such as monocytes, neutrophils and eosinophils, respond to any xenobiotic material that enters the body and generate immunity against it. A change in their normal levels is reflective of immune response to that material. In the present study, no sign of immunogenesis was observed from the hematological parameters of the rats on implantation of HGCNF3 (Table 2). Further, all the parameters lie in the range that is comparable to that of the control. This strongly affirms that HGCNF3 can be implanted into the host body as an immunocompatible biomaterial. However, thorough study on immune response of the material is quite essential before making any conclusion.

Again, toxicity of a material triggers many histological disorders. Histopathological study is therefore another vital tool for scrutinizing the host response to an implanted biomaterial. Here, a skin section gives a clear picture of normal dermatocytes with intact epidermis and dermis after 30 days of implantation (Figure 7). Similarly, liver and kidney sections showed regular arrangement of portal vein, hepatocytes and glomerulus, respectively. Normal brain cells are visible from the brain section image. Thus, a clear picture was obtained from the histopathological evaluations regarding the *in vivo* compatibility of HGCNF3. The overall study put forward HGCNF3 as a potential implant candidate for biomedical applications. However, microbial infection preventing capacity of an implant is desired to avoid postsurgical complications.

Antimicrobial Assays. MIC of the nanomaterials and nanocomposites were calculated against *S. aureus*, *E. coli* and *C. albicans*. CuO nanoparticles showed the highest inhibitory effect against all the tested strains (Figure 8). CuO based antimicrobial materials are already commercialized for their efficient activity.³⁵ Further, CuO nanoparticles were also well reported to possess excellent antimicrobial effect.³⁶ Surface activity of the nanoparticles basically causes damage to the microbes, by penetrating through their cell membranes.³⁷

However, nanohybrid formation caused a slight decrement of the MIC values against the strains. Further, indirect exposure of CuNFC suppressed the inhibitory effect to a small extent in case of the nanocomposites. However, all the materials showed significant detriment to both bacteria and fungi.

The zone inhibition assay demonstrated no effect of NFC on both bacteria and fungus. CuNFC, contrarily showed profound antimicrobial efficacy (Figure 9). HGCNF3 exhibited significant zones of inhibition in all the cases. However, the effect was stronger against the Gram-negative bacterium than the Gram-positive one and weaker against the fungus. Greater zones were observed for CuNFC than that for CuO. Exposure of the microbes to higher surface area of the nanohybrid might have affected. The above two assays confirmed the profound activity of the nanocomposite against both Gram-positive and Gram-negative bacteria as well as fungi.

Activity of the nanocomposite thermosets was analyzed against *S. aureus*, by incubating HGE and HGCNF films with the bacterium. The SEM micrographs showed clear morphological alteration of cells when incubated with the nanocomposites, whereas a contrary result was noticed for HGE. The red marks (Figure 10) indicated shrinkage and membrane disintegration of *S. aureus* cells that were adhered to HGCNF surfaces. The study confirms the ability of the material to prevent infections at surgical sites. Further, an implantable biomaterial needs biodegradability to abet repeated surgery for explantation after the completion of the service period.

In Vivo Biodegradation. Biodegradability is very essential for an implantable biomaterial, to evade repeated surgery. Geometry of the explants distorted as observed visually within 14 days. This may be due to their degradation under physiological environment. Further, SEM micrographs showed the surface degradation of the explants, which have clear distinction from the unimplanted one (Figure 11). Rate of degradation enhanced with time and granulation of tissue over the explants surfaces was observed. Surface of the explants showed erosion, which may be greatly influenced by the presence of biodegradable ether linkages in the structural backbone of HGE.²⁰ Different physiological fluids, including specific enzymes may be responsible for the degradation

process. However, more specific clinical trials are essential to draw a conclusion about the biodegradability of HGCNF3.

CONCLUSION

This study showed the advantageous attributes of the unison of polymer science and nanotechnology to fabricate an antimicrobial, biodegradable implant material. Merits of biore-source based hyperbranched epoxy and CuNFC conferred the nanocomposite high strength and flexibility as well as efficient antimicrobial property. HGCNF3 supported the growth and proliferation of L6 muscle cells, by providing a compatible surface. Cytocompatibility of the material was confirmed by incubating with rat liver cells. Moreover, HGCNF3 showed positive host response when implanted within rat host. Further, *in vivo* assay ascertained the biodegradability of the implant within host body. The overall study thus forward a biodegradable, antimicrobial, nontoxic, sustainable scaffold material for muscle tissue reconstruction. However, critical evaluation regarding biocompatibility shall be required for its eventual biomedical application.

AUTHOR INFORMATION

Corresponding Author

*N. Karak. E-mail: karakniranjan@gmail.com. Tel: + 91-3712-267009. Fax: +91-3712-267006.

Present Address

[†]Dibrugarh University, Assam, India

Author Contributions

All the authors have significantly contributed to the reported work. The final version of the paper is approved by all the authors.

Notes

The authors declare no competing financial interest.

ACKNOWLEDGMENTS

The authors express their gratitude to NRB for financial assistance through Grant no. DNRD/05/4003/NRB/251, dated 29.02.12. SAIF, NEHU, Shillong is acknowledged for the TEM imaging.

REFERENCES

- (1) Orts, W. J.; Shey, J.; Imam, S. H.; Glenn, G. M.; Guttman, M. E.; Revol, J. Application of cellulose microfibrils in polymer nanocomposites. *J. Polym. Environ.* **2014**, *13*, 301–306.
- (2) Carlsson, D. O.; Nystrom, G.; Zhou, Q.; Berglund, L. A.; Nyholm, L.; Stromme, M. Electroactive nanofibrillated cellulose aerogel composites with tunable structural and electrochemical properties. *J. Mater. Chem.* **2012**, *22*, 19014–19024.
- (3) Abdul Khalil, H. P. S.; Bhat, A. H.; Ireana Yusra, A. F. Green composites from sustainable cellulose nanofibrils: A review. *Carbohydr. Polym.* **2012**, *87*, 963–979.
- (4) Barua, S.; Das, G.; Aidew, L.; Buragohain, A. K.; Karak, N. Copper-copper oxide coated nanofibrillar cellulose: A promising biomaterial. *RSC Adv.* **2013**, *3*, 14997–15004.
- (5) Mano, J. F.; Silva, G. A.; Azevedo, H. S.; Malafaya, P. B.; Sousa, R. A.; Silva, S. S.; Boesel, L. F.; Oliveira, J. M.; Santos, T. C.; Marques, A. P.; Neves, N. M.; Reis, R. L. Natural origin biodegradable systems in tissue engineering and regenerative medicine: Present status and some moving trends. *J. R. Soc. Interface* **2007**, *4*, 999–1030.
- (6) Campbell, K. P. Three muscular dystrophies: Loss of cytoskeleton-extracellular matrix linkage. *Cell* **1995**, *80*, 675–679.
- (7) Cassell, C. S. O.; Hoferb, O. P. S.; Morrison, W. A.; Knight, K. R. Vascularisation of tissue-engineered grafts: The regulation of

angiogenesis in reconstructive surgery and in disease states. *Br. J. Plast. Surg.* **2002**, *55*, 603–610.

(8) Nikolovski, J.; Mooney, D. J. Smooth muscle cell adhesion to tissue engineering scaffolds. *Biomaterials* **2000**, *21*, 2025–2032.

(9) Dennis, R. G.; Cosnik, P. E. Excitability and isometric contractile properties of mammalian skeletal muscle constructs engineered *in vitro*. *In Vitro Cell Dev. Biol.: Anim.* **2000**, *36*, 327–335.

(10) Danielsson, C.; Ruault, S.; Simonet, M.; Neuenschwander, P.; Frey, P. Polyesterurethane foam scaffold for smooth muscle cell tissue engineering. *Biomaterials* **2006**, *27*, 1410–1415.

(11) Cheung, H.; Lau, K.; Lu, T.; Hui, D. A critical review on polymer-based bio-engineered materials for scaffold development. *Composites, Part B* **2007**, *38*, 291.

(12) Huttmacher, D. W. Scaffold design and fabrication technologies for engineering tissues -State of the art and future perspectives. *J. Biomater. Sci. Polym. Ed.* **2001**, *12*, 107–124.

(13) Mooney, D. J.; Mazzoni, C. L.; Breued, C.; McNamara, K.; Hem, D.; Vacanti, J. P.; Langer, R. Stabilized polyglycolic acid fibre-based tubes for tissue engineering. *Biomaterials* **1996**, *17*, 115–124.

(14) Drury, J. L.; Mooney, D. J. Hydrogels for tissue engineering: Scaffold design variables and applications. *Biomaterials* **2003**, *24*, 4337–4351.

(15) Koning, M.; Harmsen, M. C.; van Luyn, M. J. A.; Werker, P. M. N. Current opportunities and challenges in skeletal muscle tissue engineering. *J. Tissue. Eng. Regen. Med.* **2009**, *3*, 407–415.

(16) Chaturvedi, V.; Dye, D.; Coombe, D.; Grounds, M. Bioactive scaffolds in skeletal muscle regeneration and tissue engineering. *Aust. Biotechnol.* **2011**, *42*, 8–10.

(17) Barua, S.; Chattopadhyay, P.; Aidew, L.; Buragohain, A. K.; Karak, N. Infection-resistant hyperbranched epoxy nanocomposite as a scaffold for skin tissue regeneration. *Polym. Int.* **2015**, *64*, 303–311.

(18) Barua, S.; Dutta, N.; Karmakar, S.; Chattopadhyay, P.; Aidew, L.; Buragohain, A. K.; Karak, N. Biocompatible high performance hyperbranched epoxy/clay nanocomposite as an implantable material. *Biomater. Mater.* **2014**, *9*, 025006–025019.

(19) Petersen, N.; Gatenholm, P. Bacterial cellulose-based materials and medical devices: Current state and perspectives. *Appl. Microbiol. Biotechnol.* **2011**, *91*, 1277–1286.

(20) Barua, S.; Dutta, G.; Karak, N. Glycerol based tough hyperbranched epoxy: Synthesis, statistical optimization and property evaluation. *Chem. Eng. Sci.* **2013**, *95*, 138–147.

(21) Michael, L. F.; Wu, Z.; Cheatham, R. B.; Puigserver, P.; Adelman, G.; Lehman, J. J.; Kelly, D. P.; Spiegelman, B. M. Restoration of insulin-sensitive glucose transporter (GLUT4) gene expression in muscle cells by the transcriptional coactivator PGC-1. *Proc. Natl. Acad. Sci. U. S. A.* **2001**, *27*, 3820–3825.

(22) Franken, N. A. P.; Rodermond, H. M.; Stap, J.; Haveman, J.; van Bree, C. Clonogenic assay of cells *in vitro*. *Nat. Protoc.* **2006**, *1*, 2315–2319.

(23) Arnaoutoglou, E.; Kouvelos, G.; Milionis, H.; Mavridis, A.; Kolaitis, N.; Papa, N.; Papadopoulos, G.; Matsagkas, M. Post-implantation syndrome following endovascular abdominal aortic aneurysm repair: Preliminary data. *Interact. Cardiovasc. Thorac. Surg.* **2011**, *12*, 609–614.

(24) Barua, S.; Konwarh, R.; Bhattacharya, S. S.; Das, P.; Devi, K.S. P.; Maiti, T. K.; Mandal, M.; Karak, N. Non-hazardous anticancerous and antibacterial colloidal 'green' silver nanoparticles. *Colloids Surf., B* **2013**, *105*, 37.

(25) Wang, Y.; Kim, Y. M.; Langer, R. *In vivo* degradation characteristics of poly(glycerol sebacate). *J. Biomed. Mater. Res., Part A* **2003**, *66*, 192–197.

(26) Braunnegg, G.; Bona, R.; Koller, M. Sustainable polymer production. *Polym. Plast. Technol. Eng.* **2007**, *43*, 1779–1793.

(27) Bledzki, A. K.; Gassan, J. Composites reinforced with cellulose based fibres. *Prog. Polym. Sci.* **1999**, *24*, 221–274.

(28) Muller, F. A.; Muller, L.; Hofmann, I.; Greila, P.; Wenzelb, M. M.; Staudenmaier, R. Cellulose-based scaffold materials for cartilage tissue engineering. *Biomaterials* **2006**, *27*, 3955–3963.

(29) Mattoussi, H.; Palui, G.; Na, H. B. Luminescent quantum dots as platforms for probing in vitro and in vivo biological processes. *Adv. Drug Delivery Rev.* **2012**, *64*, 138–166.

(30) Kondo, T. The relationship between intramolecular hydrogen bonds and certain physical properties of regioselectively substituted cellulose derivatives. *J. Polym. Sci., Part B: Polym. Phys.* **1997**, *35*, 717–723.

(31) Dugan, J. M.; Gough, J. E.; Eichhorn, S. J. Bacterial cellulose scaffolds and cellulose nanowhiskers for tissue engineering. *Nanomedicine* **2013**, *8*, 287–298.

(32) Novotna, K.; Havelka, P.; Sopuch, T.; Kolarova, K.; Vosmanska, V.; Lisa, V.; Svorcik, V.; Bacakova, L. Cellulose-based materials as scaffolds for tissue engineering. *Cellulose* **2013**, *20*, 2263–2278.

(33) Das, B.; Chattopadhyay, P.; Mishra, D.; Maiti, T. K.; Maji, S.; Narayan, R.; Karak, N. Nanocomposites of bio-based hyperbranched polyurethane/functionalized MWCNT as non-immunogenic, osteoconductive, biodegradable and biocompatible scaffolds in bone tissue engineering. *J. Mater. Chem., B* **2013**, *1*, 4115–4126.

(34) Sato, Y.; Notohara, K.; Kojima, M.; Takata, K.; Masaki, Y.; Yoshino, T. IgG4-related disease: Historical overview and pathology of hematological disorders. *Pathol. Int.* **2010**, *60*, 247–258.

(35) Anyaogu, K. C.; Fedorov, A. V.; Neckers, D. C. Synthesis, characterization, and antifouling potential of functionalized copper nanoparticles. *Langmuir* **2008**, *24*, 4340–4346.

(36) Azam, A.; Ahmed, A. S.; Oves, M.; Khan, M. S.; Memic, A. Antimicrobial activity of metal oxide nanoparticles against Gram-positive and Gram-negative bacteria: A comparative study. *Int. J. Nanomed.* **2012**, *7*, 6003–6009.

(37) Barua, S.; Konwarh, R.; Mandal, M.; Gopalakrishnan, R.; Kumar, D.; Karak, N. Biomimetically prepared antibacterial, free radical scavenging poly(ethylene glycol) supported silver nanoparticles as *Aedes albopictus* larvicide. *Adv. Sci. Eng. Med.* **2013**, *5*, 291–298.